

SCC Growth Behavior of Nickel-based Alloy 600 in Safe-end Welded Joints

Zhang Jianlong^{1,3}, Cui Yinghao², Xue He¹, Lu Yuan³, Wang Shuai¹, Rehmat Bashir¹

¹ Xi'an University of Science and Technology, Xi'an 710054, China; ² Zhongyuan University of Technology, Zhengzhou 450007, China;

³ Xi'an Special Equipment Inspection Institute, Xi'an 710065, China

Abstract: Nickel-based alloys are commonly used as welding part for the primary circuit safe-end welded joints of pressurized water reactors. Due to the harsh service environment and uneven mechanical properties of the welded joints, the nickel-based alloys are prone to stress corrosion cracking, which has a great effect on the safe operation of nuclear power. To understand the effect of the material macrostructural parameters (including the plastic properties of the material and the stress intensity factor K) on the stress corrosion cracking (SCC) growth rate, the SCC propagation finite element model (FEM) of nickel-base alloy 600 under different macrostructure parameters was established, and the effects of different plasticity and K values on the plastic zone and tensile plastic strain around the crack tip were analyzed. Results show that the plastic zone size and tensile strain around crack tip are affected by K , yield strength and hardening exponent, among which the K at crack tip has a greater influence, and it is inversely proportional to yield strength, while the K is directly proportional to hardening exponent. According to the results of SCC growth rate calculated under different K and the experimental results under high-temperature water environment, the range of characteristic distance r_0 of nickel-based alloy 600 is obtained. The research results can provide a scientific basis for SCC rate prediction under high-temperature water environment of nickel-based alloy 600 for nuclear power plants.

Key words: stress corrosion cracking (SCC); nickel-based alloy; macro structural parameters; crack tip plastic zone; crack growth rate

Nickel-based alloy 600, very prone to stress corrosion cracking (SCC), is widely used in PWR nuclear power plant and dissimilar metal welded joints due to its excellent properties. And these nickel-based alloys have been served in high-temperature, high pressure and radiation for a long time^[1]. The SCC process of welded joints is a slow and stable crack propagation process determined by three factors, including corrosion medium, material properties and mechanical state at crack tip. The SCC is the main cause of failure of PWR weld material, which seriously threatens the safe operation and service life of nuclear power equipment^[2,3].

Nickel-based alloys are often used as welding consumables in safe-end welding joints of dissimilar metals. Due to the particularity of joint technique, defects such as cracks, pore, inclusions, impermeability, composition

gradient, mechanical property variation and residual stress will inevitably occur in the weld metal^[4-6]. The residual stress during welding is usually higher than the material yield strength due to thermal expansion and cold contraction of welded components, which has become the main mechanical factor causing SCC. Cold bending forming (cold working) technique is mainly used in manufacturing main pipe elbows in China. Different degrees of work hardening will occur at different sections of main pipe, and with increasing the wall thickness of main pipe, the cold bending deformation rate (work hardening) will gradually increase. Relevant research has shown that cold working can promote SCC and accelerate SCC crack growth rate^[7,8]. Moreover, it is difficult for metal materials to be in an ideal elastic-plastic state in

Received date: May 26, 2019

Foundation item: National Natural Science Foundation of China (51811530311)

Corresponding author: Xue He, Ph. D., Professor, School of Mechanical Engineering, Xi'an University of Science and Technology, Xi'an 710054, P. R. China, Tel: 0086-29-85583159, E-mail: xue_he@hotmail.com

Copyright © 2020, Northwest Institute for Nonferrous Metal Research. Published by Science Press. All rights reserved.

practical engineering, and the influence of material plastic properties on SCC should also be considered.

Stress intensity factor K characterizes the strength of the stress field near the crack tip, and at the same time, the crack growth rate has a strong correlation with K ^[9]. The zone around the crack tip will form a plastic zone before fracture occurs, and the plastic zone size around the crack tip directly affects the crack initiation, crack growth rate and instability fracture, which is also an important parameter for characterizing the material fracture^[10-12].

The research mentioned above shows that during the process of crack initiation and propagation, there is a close relationship between SCC growth and the change of plastic zone around crack tip and K , material yield strength and hardening exponent. Therefore, the finite element analysis model of nickel-base alloy 600 was established using ABAQUS, and the relationship between plastic zone around crack tip, material plasticity and stress intensity factor K was analyzed. The influence of material plasticity and stress intensity factor on the SCC growth rate was also predicted. On this basis, the range of relative reasonable characteristic distance r_0 for nickel-base alloy 600 was obtained by comparing the SCC growth rate experiment in high-temperature water environment.

1 Theoretical Model for SCC Quantitative Prediction

F-A model was established by Ford and Andresen of General Corporation^[13], which is widely used in high-temperature water environment based on the theory of slip dissolving film rupture. The specific expression of the model is shown in Eq.(1).

$$\frac{da}{dt} = \kappa_a (\dot{\epsilon}_{ct})^m \tag{1}$$

where m is the exponent of current decay curve, which is related to the corrosion potential, solution conductivity and chromium depletion; $\dot{\epsilon}_{ct}$ is the strain rate at crack tip; κ_a is the oxidation rate constant, which is determined by the environment and material in the vicinity of the crack tip, and it is given as follows:

$$\kappa_a = \frac{M}{\rho F z} \frac{i_0}{1-m} \left(\frac{t_0}{\epsilon_f} \right)^m \tag{2}$$

where M is the metal molecular mass; ρ is the metal density; F is the Faraday's constant; z is the change in charge during the oxidation process; i_0 is the oxidation current density of the bare surface; t_0 is the time before onset of the current decay and ϵ_f is the oxide film degradation strain.

Considering that it is difficult to obtain the strain rate at the crack tip by the F-A model, a crack-tip strain rate model based on the theory of crack-tip strain gradient was deduced by Professor Shoji^[14] of Japan Northeast University, and is shown in Eq.(3), where E is the Young's modulus and N is

the strain hardening exponent in Gao Hwang field. FRI model establishes the relationship between crack tip strain rate and macro-mechanical parameters, which has been adopted by many laboratories around the world. Meanwhile, engineering applications have also been achieved to some extent, but the crack tip characteristic distance r_0 in the model has not yet been clearly defined.

$$\dot{\epsilon}_{ct} = \beta \frac{\sigma_{ys}}{E} \frac{N}{N-1} \left(\frac{\dot{a}}{K} \right) \left[\ln \left(\frac{R_p}{r_0} \right) \right]^{\frac{1}{N-1}} \tag{3}$$

To obtain the strain rate at the crack tip, Xue et al^[15] proposed an alternative algorithm of the strain rate at the crack tip, that is, the plastic strain at r_0 in front of the crack tip is used to replace the strain at the crack tip, as shown in Eq.(4), where r_0 is a distance from the crack tip.

$$\epsilon_{ct} = \epsilon_p \Big|_{r=r_0} \tag{4}$$

the variation of the distance r will cause the increase of crack tip strain when the crack propagates.

$$\dot{\epsilon}_{ct} = \dot{\epsilon}_p = \frac{d\epsilon_p}{da} \cdot \frac{da}{dt} \tag{5}$$

where, $d\epsilon_p/da$ is the strain rate at a characteristic distance r_0 in front of the growing crack tip.

Substituting Eq.(5) into Eq.(1), the SCC growth rate at crack tip in a high-temperature water environment can be expressed as follows:

$$\frac{da}{dt} = \kappa_a' \left(\frac{d\epsilon_p}{da} \right)^{\frac{m}{1-m}} \tag{6}$$

$$\text{where } \kappa_a' = (\kappa_a)^{\frac{1}{1-m}} \tag{7}$$

For a stable propagation crack tip, Eq.(5) can be expressed as Eq.(8), and the calculation method of the tensile plastic strain rate at the crack tip is shown in Fig.1.

$$\frac{d\epsilon_p}{da} = - \frac{d\epsilon_p}{dr} \tag{8}$$

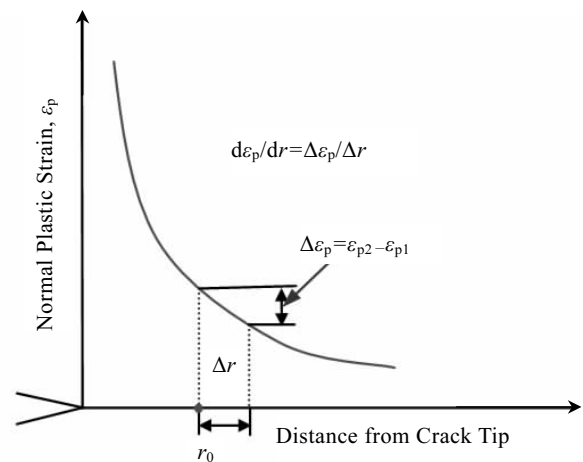


Fig.1 Acquisition of plastic strain rate in front of crack tip by numerical simulation

Substituting Eq.(8) into Eq.(6) can obtain the expression of SCC growth rate, as shown in Eq.(9).

$$\frac{da}{dt} = \kappa_a \left(\frac{d\varepsilon_p}{dr} \right)^{\frac{m}{1-m}} \quad (9)$$

It can be seen from the SCC growth model that the characteristic distance r_0 in front of crack tip is an important parameter affecting the crack growth rate and the stress corrosion mechanism. Based on the elastic-plastic finite element method (EPFEM) and the calculation principle of Fig.1, the plastic deformation at the characteristic distance r_0 in front of the crack tip can be calculated, and then the crack growth rate can be obtained according to the plastic strain rate. In this study, by analyzing the effect of macrostructure parameters on the size of plastic zone at the crack tip and the crack growth rate of nickel-based alloy 600, including material plasticity and stress intensity factor, a more accurate range of characteristic distance can be obtained to further improve the accuracy of the model.

2 Finite Element Model

2.1 Geometric and material model

Nickel-based alloy is one of the common materials used in safe-end welded joints, and it is easy to cause SCC when severed in high-temperature water environment. To understand the influence of macro-structural parameters (including material plasticity and stress intensity factor) on the growth rate of SCC, CT specimen with defects is adopted as a geometric model in this research. The geometric shape and size of the specimens conform to the ASME-E399 standard. Meanwhile, the width of the specimen is $W=25.4$ mm and the crack length is $a=11.25$ mm.

The research object is nickel-base alloy 600 in this study, which is a power hardening material. The relationship between stress and strain can be described using the Ramberg-Osgood model, as shown in Eq.(10)^[16]:

$$\frac{\varepsilon}{\varepsilon_0} = \frac{\sigma}{\sigma_0} + \alpha \left(\frac{\sigma}{\sigma_0} \right)^n \quad (10)$$

where ε is the total strain, including elastic and plastic strain; σ is the total stress; ε_0 is the material yield strain; σ_0 is the material yield stress; α is the offset coefficient and n is the strain hardening exponent. The mechanical properties of the material in high-temperature water at 340 °C are shown in Table 1.

On the basis of the basic data, the material plastic properties will change because the welded zone is affected by the welded joint inhomogeneity. To understand the effect of material plastic change of nickel-based alloy 600 on SCC crack tip mechanics field and SCC growth rate in detail, the yield strength was set as 300, 500 and 700 MPa. When studying the influence of hardening exponent n on SCC growth rate, n is set to 4, 6 and 8. According to the general range of K in stress corrosion cracking process^[18], the values of K are set to be 10, 20 and 30 MPa·m^{1/2}.

2.2 Finite mesh model

The typical finite element mesh model in Fig.2b contains 6043 8-node biquadratic plane strain elements, where x -coordinate is the crack growth direction and y -coordinate is the normal direction of crack in the coordinate system. In order to understand the detail of the stress and strain close to the crack tip, a small size blunt notch with 1 μ m in radius is designed at the crack tip and the vicinity zone of the crack tip is significantly refined. 1526 8-node biquadrate plane strain quadrilateral elements are adopted, which is shown in Fig.2c.

Table 1 Mechanical properties of nickel-base alloy 600 and its oxide formed in PWR primary water at 340 °C^[17]

| Material parameter | Value |
|---------------------------------|---------|
| Young's modulus, E /MPa | 189 500 |
| Poisson's ratio, ν | 0.286 |
| Yield strength, σ_0 /MPa | 436 |
| Yield offset, α | 3.075 |
| Hardening exponent, n | 6.495 |

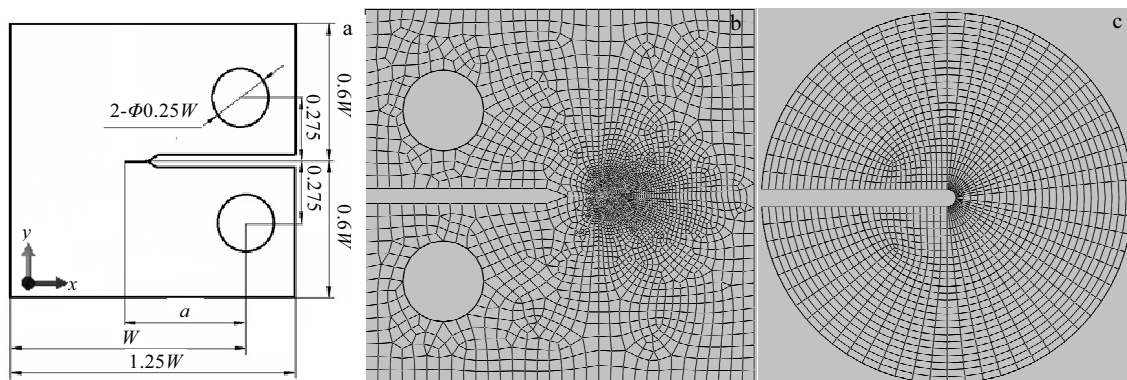


Fig.2 Finite element model: (a) geometric model, (b) global mesh specimen, and (c) local crack front mesh model

3 Results and Discussion

3.1 Effect of macrostructural parameters on plastic zone size

The plastic zone size in front of the crack tip is an important parameter used in the quantitative prediction of the SCC crack growth rate. Based on von Mises yielding principle, the plastic zone size R_p in front of the crack tip is shown in Fig.3, which shows that the plastic zone size R_p will increase as stress intensity factor K increases, and simultaneously, the plastic zone size R_p also increases as the material yield strength decreases, and when the yield strength of material is low, the size of plastic zone is obviously affected by stress intensity factor. It can be seen from Fig.4 that the effect of hardening exponent on the plastic zone size is contrary to that of the yield strength. The plastic zone size at crack tip increases with increasing the hardening exponent under the same K .

The plastic zone size R_p extension induced by the material plasticity will availably release the stress intensity close to the crack tip under a constant K , and accordingly decrease the SCC crack growth rate.

3.2 Effect of material plasticity and K on tensile strain in front of the crack tip

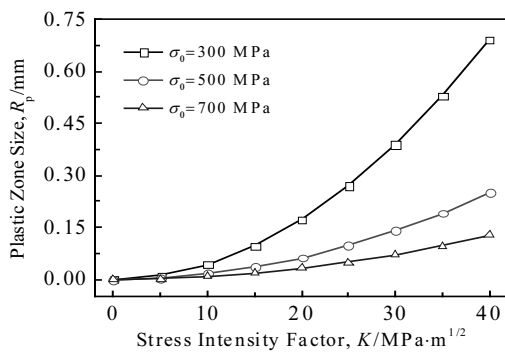


Fig.3 Distribution of plastic zone size under different yield stresses

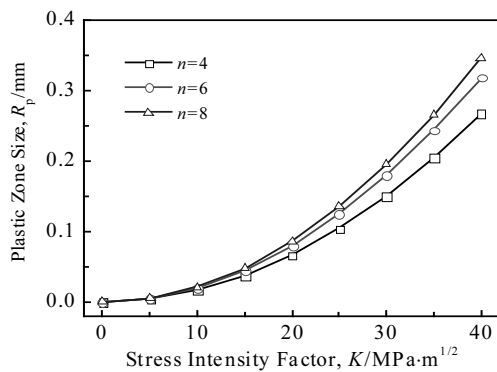


Fig.4 Distribution of plastic zone size under different hardening exponents

The distribution of tensile strain at different distances in front of crack tip of nickel-base alloy under different yield strengths is shown in Fig.5, which shows that the tensile strain of crack tip decreases with the increase of yield strength, and the larger the distance from the crack tip, the lower the tensile plastic strain. Through the influence of yield strength on the tensile plastic strain in front of the crack tip, it can be concluded that the lower the yield strength of nickel-based alloy material, the greater the plastic deformation in front of the crack tip, which will easily lead to the oxide film rupture at the crack tip and accelerate crack growth rate.

Tensile strain distribution at different distances in front of the crack tip of nickel-based alloys under different hardening exponents is shown in Fig.6, which shows that the tensile strain at the crack tip increases with the increase of material hardening exponent. At the same time, tensile plastic strain becomes lower and lower with increasing the distance to the crack tip under different hardening exponents. Through the influence of hardening exponent on the tensile plastic strain in front of crack tip, it can be concluded that tensile plastic deformation of crack tip increases with the increase of hardening exponent, which will easily lead to cracking of oxide film at crack tip and accelerate crack growth rate. Comparison shows that the effect of hardening exponent on tensile strain at the crack tip is opposite to the effect of yield strength on the tensile strain.

The tensile strain distribution at different distances in front of the crack tip under different stress intensity factors is shown in Fig.7. The tensile strain in front of the crack tip, as one of the main driving forces leading to the cracking of oxide film, is greatly affected by the distance to the crack tip. With the increase of the distance from the front of the crack tip, the tensile strain decreases gradually under a constant K . At the same characteristic distance r_0 , the greater the stress intensity factor at the crack tip, the

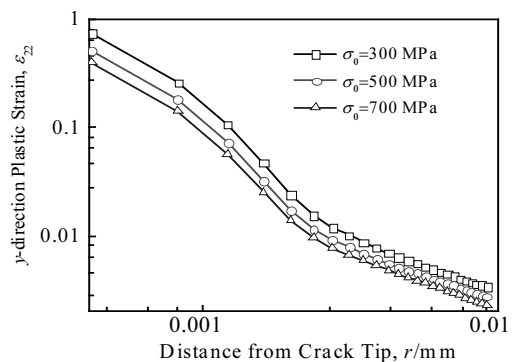


Fig.5 Tensile strain ahead of the crack tip under different yield stresses

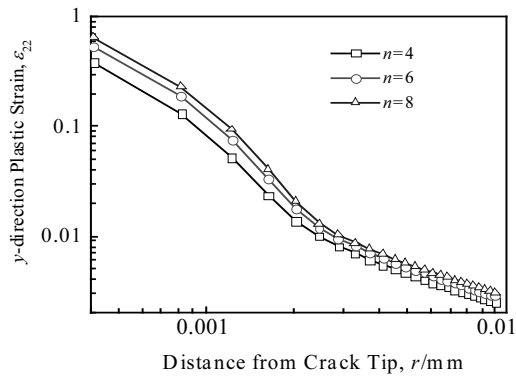


Fig.6 Tensile strain ahead of the crack tip under different hardening exponents

greater the tensile plasticity at the crack tip, and the larger the strain, the slower the increasing trend with the increase of the K . It can be seen from the comparison that the increase of K at crack tip will lead to the increase of plastic strain, which will accelerate the crack growth rate of SCC.

3.3 Effect of material plasticity and K on the crack growth rate of alloy 600

The SCC crack growth rate calculation model shows that crack growth rate is closely related to the tensile strain rate at the characteristic distance r_0 from the front of the crack tip. The plastic strain rate changes at r_0 under different characteristic distances to the crack tip are calculated by the calculation method given in Fig.1, and then the numerical results of $d\varepsilon_{22}/dr$ are substituted into Eq.(9) to obtain the change of the growth rate.

The hydro-chemical parameters of nickel-based alloy 600 in high-temperature water environments are shown in Table 2, and through calculation we can derive that the oxidation rate constant κ_a' is 7.478×10^{-7} .

According to the range of r_0 in Ref. [19], the SCC crack growth rate at different r_0 under different yield strengths is

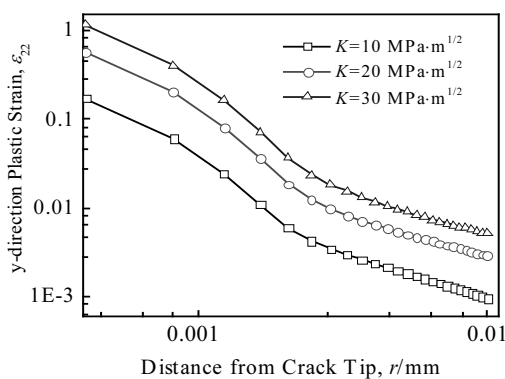


Fig.7 Tensile strain ahead of the crack front under different K

Table 2 Water chemistry material parameter of alloy 600^[15]

| Parameter | Value |
|---|----------|
| Atomic mass, $M/g\cdot mol^{-1}$ | 55 |
| Number of equivalents exchanged, z | 2.67 |
| Oxidation current density, $i_0/A\cdot mm^{-2}$ | 0.000 15 |
| Fracture strain of oxide film, ε_f | 0.0025 |
| Exponent of current decay curve, m | 0.4 |
| Faraday's constant, $F/C\cdot mol^{-1}$ | 96 500 |
| Duration of constant i_0 , t_0/s | 0.4 |
| Density, $\rho/g\cdot mm^{-3}$ | 0.007 86 |

shown in Fig.8. The crack growth rate is the largest at 3 μm ahead of the crack tip, and the maximum tensile plastic strain rate appears at the crack tip. With the increase of the characteristic distance r_0 , the crack growth rate decreases gradually. The yield strength has a great influence on the crack growth rate. The SCC crack growth rate of materials with high yield strength is relatively low. In the range of crack characteristic distance of 3~10 μm , the crack growth rate ranges from 2.4×10^{-7} mm/s to 2.4×10^{-6} mm/s.

Fig.9 shows the distribution curve of crack growth rate of nickel-base alloy 600 under different characteristic distances r_0 in front of the crack tip. It can also be seen that the crack growth rate is the largest at 3 μm ahead of crack tip, and the crack tip has the largest tensile plastic strain rate at this time. With the increase of characteristic distance r_0 , the crack growth rate decreases gradually. Moreover, different K values have a great influence on the crack growth rate. The greater the stress intensity factor K , the higher the SCC crack growth rate. It is mainly due to the increase of K , which leads to the increase of plastic strain rate in front of the crack tip. At the same characteristic distance, the variation range of crack growth rate is larger than that of yield strength, ranging from 1.0×10^{-7} ~ 3.2×10^{-6} mm/s.

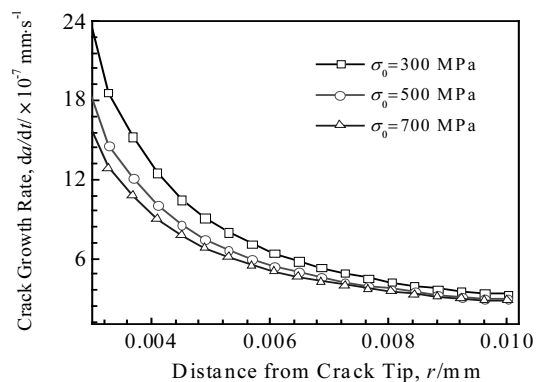


Fig.8 Crack growth rate ahead of crack tip under different yield stresses

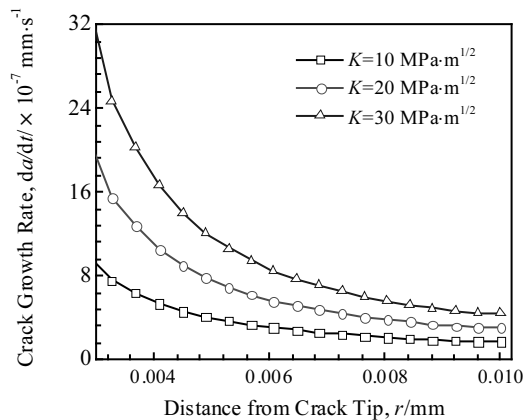


Fig.9 Crack growth rate ahead of crack tip under different K

Fig.10 shows the distribution curve of the crack growth rate of nickel-base alloy 600 at different characteristic distances r_0 under different hardening exponents. The influence law of characteristic distance r_0 on crack growth rate is consistent with that of yield strength and K . The crack growth rate increases with the increase of material hardening exponent at the same crack characteristic distance r_0 . Meanwhile, the crack growth rate varies from $2.5 \times 10^{-7} \sim 2.1 \times 10^{-6}$ mm/s.

3.4 Comparison of crack growth rate results based on EPFEM and experiment in high-temperature water environment

Based on the influence of stress intensity factor on crack growth rate, we can derive that different characteristic distances r_0 have great influence on crack growth rate, and the SCC growth rate is close to two orders of magnitude under different r_0 . To further improve the prediction ability of the SCC growth rate prediction model based EPFEM, the SCC experimental results are compared with the results from prediction model of Eq.(9) under different K .

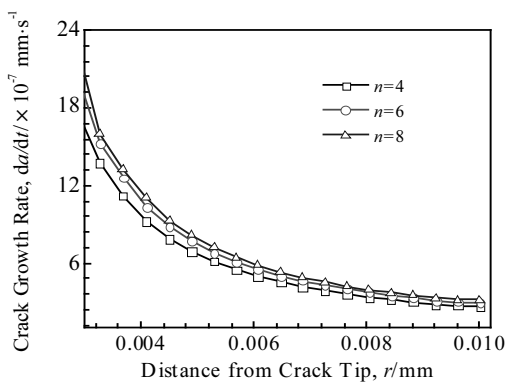


Fig.10 Crack growth rate ahead of crack tip under different n

Fig.11 shows the comparison of the experiment results and model predicted result based on EPFEM. From the experimental results^[20], it can be derived that the value of crack growth rate has a great dispersion under the same stress intensity factor K . According to the prediction model of different r_0 under the K value of $20 \text{ MPa}\cdot\text{m}^{1/2}$, it can be concluded that the crack growth rate variation ranges from 1.0×10^{-7} mm/s to 3.2×10^{-6} mm/s when the r_0 value is $3 \sim 10 \mu\text{m}$. When the value of K is $20 \text{ MPa}\cdot\text{m}^{1/2}$, the crack growth rate value is $7.65 \times 10^{-7} \sim 1.22 \times 10^{-6}$ mm/s based on the SCC experiment result. According to the comparison of crack growth rate values measured by experiments under the same stress intensity factor, we can conclude that when the characteristic distance r_0 is $3.5 \sim 5.5 \mu\text{m}$ from the front of the crack tip, the experimental results are of the same order of magnitude as SCC predicted results based on the model.

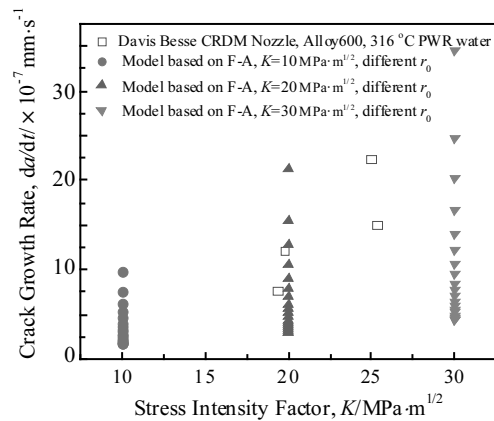


Fig.11 Comparison of experimental data and model predicted rate under different stress intensity factors

4 Conclusions

1) The increase of stress intensity factor K will improve the plastic zone size at the crack tip and the SCC crack growth rate. The decrease of material yield strength or the increase of hardening exponent can also cause the increase of plastic zone size at crack tip.

2) Tensile plastic strain decreases with increasing the distance from the crack tip. Meanwhile, the higher the hardening exponent n and stress intensity factor K , the larger the plastic deformation in front of the crack tip, which can easily lead to the rupture of crack tip oxide film and accelerate the crack growth rate, while the change of yield strength has the opposite effect on the tensile plastic strain.

3) The crack growth rate is the highest at $3 \mu\text{m}$ from the crack tip. With the increase of the characteristic distance r_0 , the crack growth rate decreases gradually. The range of the characteristic distance r_0 of nickel-based alloy 600 is

obtained by comparing the calculated SCC growth rate using prediction model with the SCC experiment result under a high-temperature water environment, and a more reasonable scope of r_0 of 3.5~5.5 μm is determined for nickel-based alloy 600 in prediction model.

References

- Dong L J, Peng Q J, Xue He et al. *Corrosion Science*[J], 2018, 60(132): 9
- Tice D R. *Corrosion Science*[J], 1985, 25(8-9): 705
- Peng Q J, Hou J, Yonezawa T et al. *Corrosion Science*[J], 2012, 57(1): 81
- Tsuruta T, Sato K, Asada S et al. *PWSCC of Nickel Base Alloys in Vapor Phase Environment of Pressurizer*[C]. Florida: International Conference on Nuclear Engineering, 2008: 571
- Chung W C, Huang J Y, Tsay L W et al. *Materials Transactions*[J], 2011, 52(1): 12
- Li G F, Congleton J. *Corrosion Science*[J], 2000, 42(6): 1005
- Gu X D. *Selected Collection of Advanced Technology of Pressure Vessel in the Sixth National Pressure Vessel Academic Conference*[C]. Beijing: Chinese Mechanical Engineering Society, 2005: 5 (in Chinese)
- Du D, Chen K, Yu L et al. *Journal of Nuclear Materials*[J], 2015, 456: 228
- Lu Z, Shoji T, Meng F et al. *Corrosion Science*[J], 2011, 53(1): 247
- Huang J, Yang B C. *Journal of Transport Science and Engineering*[J], 2010, 26(4): 35
- Rodrigues D M, Antunes F V. *Engineering Fracture Mechanics*[J], 2009, 76(9): 1215
- Paul S K. *Theoretical and Applied Fracture Mechanics*[J], 2016, 84: 183
- Ford P. *International Journal of Pressure Vessels and Piping*[J], 1989, 40(55): 343
- Shoji T, Lu Z, Murakami H. *Corrosion Science*[J], 2010, 52(3): 769
- Xue H, Sato Y, Shoji T. *Journal of Pressure Vessel Technology*[J], 2009, 131(1): 3 027 458
- Ramberg W, Osgood W R. *Tech Note*, 902[R]. Washington: NACA, 1943
- Fang X R, Yang J H, Shao Y R et al. *Rare Metal Materials and Engineering*[J], 2019(8): 2425
- Toivonen A. *VTT Technical Research Centre of Finland*[M]. Espoo: VTT publications, 2004
- Peng Q J, Kwon J, Shoji T. *Journal of Nuclear Materials*[J], 2004, 324(1): 52
- Aly O F, Mattar N, Miguel M et al. *International Nuclear Atlantic Conference* [C]. BeloHorizonte: Technical Contribution to 64th ABM Annual Congress, 2009

安全端焊接接头镍基合金 600 应力腐蚀裂纹的扩展行为

张建龙^{1,3}, 崔英浩², 薛河¹, 鲁元³, 王帅¹, Rehmat Bashir¹

(1. 西安科技大学, 陕西 西安 710054)

(2. 中原工学院, 河南 郑州 450007)

(3. 西安特种设备检验检测院, 陕西 西安 710065)

摘要: 镍基合金作为压水堆一回路安全端焊接接头焊缝的常用材料, 由于严苛的服役环境以及焊缝处材料力学性能的不均匀使得镍基合金极易发生应力腐蚀开裂 (SCC) 现象, 对核电安全运行造成很大影响。为了解材料宏观结构参量变化 (包括材料塑性性能以及应力强度因子 K) 对 SCC 裂纹扩展速率的变化, 通过建立镍基合金 600 在不同宏观结构参量下的 SCC 裂纹扩展有限元模型, 分析了镍基合金 600 不同塑性以及载荷参数变化对裂尖塑性区和拉伸塑性应变的影响。结果表明: 塑性区尺寸及裂尖拉伸应变受到裂尖应力强度因子、屈服强度及硬化指数的影响, 其中裂尖应力强度因子的影响较大, 同时与屈服强度成反比, 应力强度因子和硬化指数成正比; 通过比较不同应力强度因子下计算所得 SCC 扩展速率结果和高温水环境下 SCC 扩展速率实验, 获得了符合镍基合金 600 的特征距离 r_0 的取值范围。研究结果能为核电镍基合金 600 在高温水环境下 SCC 速率预测提供一定的科学依据。

关键词: 应力腐蚀开裂; 镍基合金; 宏观结构参量; 裂尖塑性区; 裂纹扩展速率

作者简介: 张建龙, 男, 1988 年生, 博士生, 西安科技大学机械工程学院, 陕西 西安 7100154, E-mail: jlzhang916@hotmail.com